Future Journal of Pharmaceutical Sciences

RESEARCH

Open Access

Synthesis, antimicrobial evaluation, and *in silico* studies of some novel hydrazinylquinoline and pyrazoline derivatives as potential antimicrobial agents

Rabiu Bako[1,8*], Natasha October[2], Abdullahi Yunusa Idris[3], Asma'u Nasir Hamza[3], Gbonjubola Olusesi Adeshina[4], Ahmed Rufa'i[5], Isah Jamiu Muhammad[6] and Yahaya Yakubu[7]

Abstract

Antimicrobial resistance remains a major global public health challenge, contributing to increased mortality rate and treatment failures in an effort to address this growing challenge, the present research work focused on the synthesis and evaluation of new hydrazone scaffold and pyrazoline derivatives (coded HS6–HS10) as potential antimicrobial agents. The target compounds were synthesized via one-pot condensation reactions and characterized using FTIR, ^{1}H, and ^{13}C NMR techniques. Their antimicrobial activities were assessed *in vitro* against a panel of Gram-positive, Gram-negative bacteria, and fungal strains. However, their assessment revealed broad spectrum of antimicrobial activity, where the compounds bearing biaryl-substituted hydrazones with electron-donating or electron-withdrawing groups at para- and or meta-positions showed highest potency. However, MIC values of 12.5 mg/mL were observed against clinical isolates such as *E. coli*, *S. typhi*, and *P. aeruginosa*, while *S. aureus*, *B. subtilis*, and *S. pneumoniae* were inhibited at 12.5–25 mg/mL, while MIC values of 50 mg/mL were recorded against *Aspergillus niger*, indicating weak antifungal activity. The molecular docking studies conducted using target microbial enzymes such as dihydrofolate reductase (DHFR) and squalene epoxidase (SQLE) against the ligands HS7 and HS8 have strong binding affinities towards DHFR (− 9.6 and − 9.4 kcal/mol) and SQLE (− 9.8 and − 10.2 kcal/mol), respectively, outperforming standard reference drugs ciprofloxacin (− 7.4 kcal/mol) and terbinafine (− 9.8 kcal/mol). Meanwhile, the *in silico* ADME analysis confirmed that all compounds satisfied Lipinski's rule of five, suggesting favourable drug-like properties. In conclusion, these findings suggest that substituted hydrazone and pyrazoline derivatives possess considerable promising scaffolds for developing better novel antimicrobial agents that are capable of combating resistant pathogens.

Keywords Phenylhydrazone, Antibacterial agent, Antifungal agent, Inhibition zone, MBC, MFC, MIC, DHFR, SQLE

*Correspondence:
Rabiu Bako
rabiu.bako@kasu.edu.ng
Full list of author information is available at the end of the article

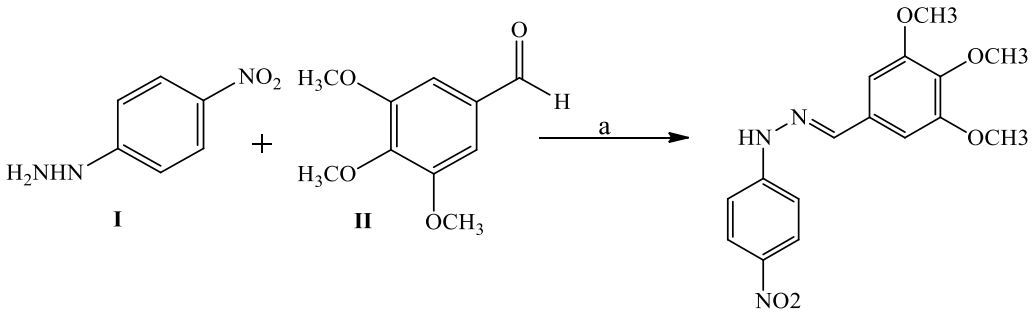

Scheme 1 Synthesis of the target compounds HS6 & reagents and conditions: EtOH, CH_3CO_2H, reflux, 3h

Introduction

Microorganisms are widespread in nature; some are beneficial, while some are pathogenic and cause serious harm to humans; this includes bacteria, fungi, viruses, algae, protozoa, etc. [1]. Pathogenic infections are the main agent leading to increase in morbidity and mortality rates across the globe [2]. Antimicrobial resistance was discovered to be among serious public health problem misuses and over uses antibiotics drugs [3]. It was also reported that modification of the current drug structure or designing new compounds with two or more targets may be a promising solution to drug resistance challenges [4]. Clinically, studies have shown that the use of antimicrobial agents such as chelation agents helps in the treatment of pathogenic infectious diseases [5]. Quinoline phenylhydrazone and pyrazoline derivatives can act as chelating agents due to the presence of carbonyl and electron-withdrawing groups attached to the molecule. The antimicrobial effects of the azole derivatives have been reported previously by Sadeghian et al., who demonstrated that 3-hydroxypyridin-4-one derivatives were effective chelating agents which could be good antimicrobial drug candidates for the treatment of *Escherichia coli, Pseudomonas aeruginosa, Bacillus subtilis, and Staphylococcus aureus* [5], whereas hydrazones and their analogues possess an azomethine functional group which was reported to have high chances for having various biological activities such as antimicrobial, antifungal, etc. [6]. Pyrazoline can be described as a five-membered ring heterocyclic compounds that possess prominent pharmacological activities such as antimicrobial, anticancer, antimalarial activities, etc. [7, 8]. Designing new antimicrobial agents of hybrid derivatives such as phenylhydrazone and pyrazoline scaffolds may be a significant contribution to address the limitations posed by existing antimicrobial drugs.

Material and method

Chemicals and instrument

All the solvents and reagents used for this research work are of analytical grade such as 4,7-chloroquinoline, substituted acetophenone, hydrazine hydrate, and some organic solvents which include acetone, absolute ethanol, chloroform ($CHCl_3$), and dichloromethane (DCM). However, the glassware used for antimicrobial experiments was sterilized using *(Autoclave*) and dry off at 60 °C for 30 min in an oven before used [9].

Methodology

General synthesis of phenylhydrazone and pyrazoline derivatives

Synthesis of (E)-1-(4-nitrophenyl)-2-(3,4,5-trimethoxybenzylidene) hydrazine (HS6)

A mixture of one mole equivalent of 3,4,5-trimethoxybenzyldehyde (**II**) (0.5 g, 5 mmol) and phenyl hydrazine (**I**) (0.5 ml, 5 mmol) was dissolved in 30 ml ethanol and stirred homogenously followed by drop-wise addition of glacial acetic acid, and the resultant mixture was refluxed for 3 h at 65 °C [10]. The progress of the reaction was monitored by thin-layer chromatography (TLC) using hexane: ethyl acetate (7:3) as the eluent. Upon completion, the reaction mixture was filtered under vacuum filtration and dried to obtained the desire product [11, 12] (Scheme 1).

Synthesis of (E)-7-chloro-4-(2-(1-(4-fluorophenyl) ethylidene) hydrazinyl) quinoline (HS7–HS8)

A mixture of one mole equivalent of hydrazinoquinoline (**IV**) was prepared by dissolving 4, 7- chloroquinoline (**III**) (0.99 g, 5 mmol) in ethanol (10 ml). To the stirred solution, hydrazine hydrate (10 ml, 5 mmol) was added and allowed to stir at 80 °C for 2 h under reflux. Upon completion, the isolated crude intermediate product

(**IV**) (0.2 g, 1 mmol) was added to a stirred solution of the appropriate substituted aldehyde (**V**) (0.1 g, 1 mmol) in ethanol (ml). The resultant homogenous mixture was refluxed for 4-16 h and monitored using thin-layer chromatography (TLC) [13, 14] (Scheme 2).

Synthesis of (E) 1-(3-(4-fluorophenyl)-5-(4-hydroxy-3-methoxyphenyl)-4,5-dihydro-1H-pyrazol-1-yl)ethanone (HS9–HS10)

The synthesis of the above compound was performed by conventional method where an appropriate substituted acetophenone (VI) (0.82 g, 5 mmol) in absolute ethanol (20 ml), vanillin (VII) (0.76 g, 5 mmol) were added, in round bottle flask containing 30 ml of ethanol with 40% (w/v) NaOH (20 ml). The reaction mixture was refluxed at 70 °C for 4 h, and the final crude product was poured into cold ice crush and neutralized with HCl 10% (v/v) to obtain the chalcone (VIII) [15]. In the subsequent step, the appropriate chalcone (VIII) (0.15 g, 1 mmol) was dissolved in glacial acetic acid (10 ml) followed the addition of hydrazine hydrate (0.2 ml, 4 mmol). The overall mixture was stirred under reflux at 60–75 °C for 6 h. The reaction mixture was monitored using TLC plate, and the vacuum filtration of the mixture is obtained as solid precipitate [16]. The pyrazoline derivatives were synthesized according to the synthesis pathway shown in Scheme 3.

Antimicrobial evaluation of the synthesized compounds

The synthesized compounds of phenylhydrazone and pyrazoline derivatives were screened out for antimicrobial evaluation.

Source of test organisms

The clinical isolate was obtained from Ahmadu Bello University Teaching Hospital (ABUTH) Shika, and pure isolate of *Staphylococcus aureus* (SA), *Escherichia coli* (EC), *Streptococcus pneumoniae* (SP), *Bacillus subtilis* (BS), *Salmonella typhi* (ST), *Aspergillus niger* (AN), and *Pseudomonas aeruginosa* (PS) was standardized from Department of Pharmaceutical microbiology Laboratory, Faculty of Pharmaceutical Sciences, at Ahmadu Bello University (ABU), in Zaria.

Preparation of inoculum

The microbial cultures were periodically sub-cultured in Nutrient broth for bacterial cultures while potato

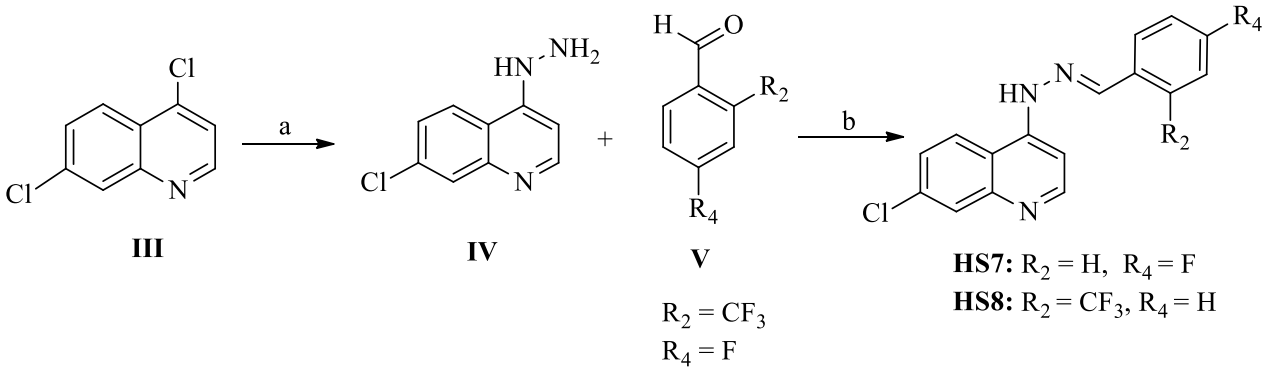

Scheme 2 Synthesis of the target compounds HS7–HS8. Reagents and conditions: **a** NH_2-NH_2.H_2O, EtOH, reflux, 2h; **b** EtOH, reflux, 4h

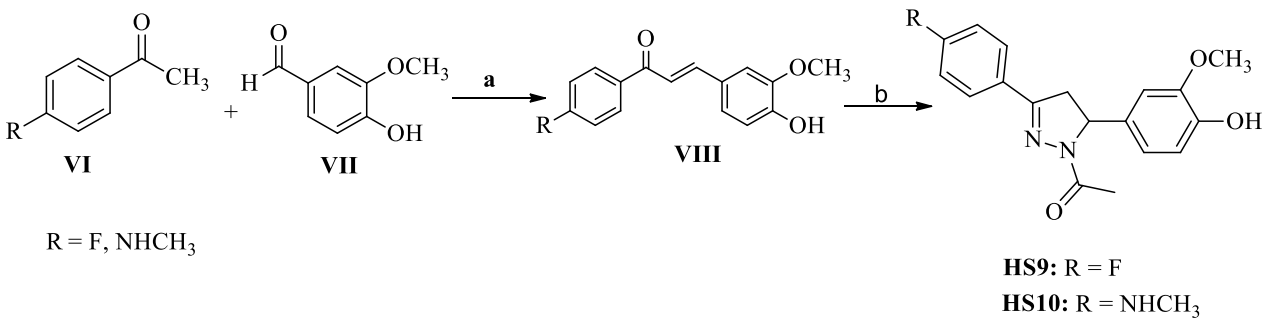

Scheme 3 Synthesis of the target compounds HS9–HS10 & reagents and conditions: **a** EtOH, 40% NaOH, reflux, 4h at 70°C, **b** CH_3COOH, NH_2NH_2.H_2O, reflux, 3h; 60–75°C

dextrose broth for fungal cultures, and the cultures were grown overnight in the respective medium [17].

Preparation of test sample

All the glassware used for the experiments was sterilized using autoclave and dried off at 60 °C for 30 min in an oven before use [9]. The five (5) test compounds were prepared by dissolving in dimethyl sulphoxide (DMSO) and mixed with tween 80, at concentrations of 50 µg/mg, 25 µg/mg, 12.5 µg/mg, and 6.25 µg/mg for testing zone of inhibition while 12.5 µg/mg, 6.25 µg/mg, 3.125 µg/mg, and 1.5625 µg/mg were subsequently used for determination of MIC, MBC, and MFC.

Determination of antimicrobial activity (zone of inhibition)

The synthesized phenylhydrazones and pyrazolines were evaluated in testing their antibacterial and antifungal activity by measuring the zone of inhibition for each bacterial culture used in this research work using agar well diffusion method. However, the bacterial strains were cultured on the Mueller–Hinton Agar (MHA) and the fungal strains on the potato dextrose agar (PDA) media plate [9]. The sterile cork borer of 6 mm diameter was used to make wells on the prepared medium, and 1 mL of the synthetic compound was dropped into the well and the plates were then incubated at 37 °C for 24 h. However, after the incubation period, the diameters with no growth of the inoculated microorganisms (inhibition zones) around the well

Table 1 Structures of the designed library of phenyl, quinoline hydrazone derivatives

Compound code	2D-representation/IUPAC name	Novelty status
HS6	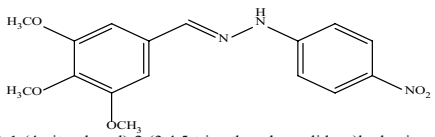 (*E*)-1-(4-nitrophenyl)-2-(3,4,5-trimethoxybenzylidene)hydrazine	New
HS7	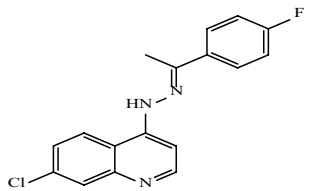 (*E*)-7-chloro-4-(2-(1-(4-fluorophenyl)ethylidene)hydrazinyl)quinoline	New
HS8	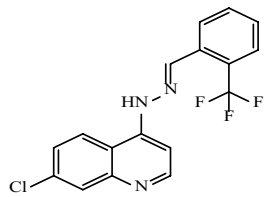 (*E*)-7-chloro-4-(2-(1-(2-trifluoromethyl)phenyl)ethylidene)hydrazinyl)quinoline	New
HS9	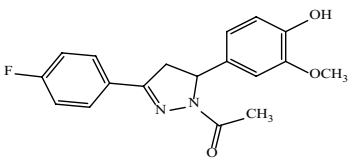 1-(3-(4-fluorophenyl)-5-(4-hydroxy-3-methoxyphenyl)-4,5-dihydro-1H-pyrazol-1-yl)ethanone	New
HS10	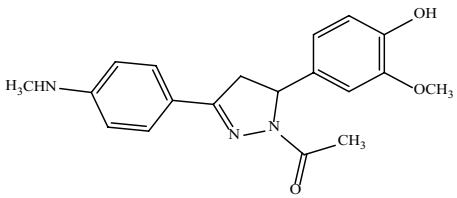 1-(5-(4-hydroxy-3-methoxyphenyl)-3-(4-(methylamino)phenyl)-4,5-dihydro-1H-pyrazol-1-yl)ethanone	New

were measured with ruler in millimetres, and the mean values were calculated as shown in Table 1 below [18]. Ciprofloxacin and terbinafine were used as reference drugs for antibacterial and antifungal, respectively, with complete growth inhibition of the test organism [19].

Determination of minimum inhibitory concentration (MIC)

Minimum inhibitory concentration (MIC) is the least concentration of an antimicrobial agent that would inhibit the visible growth of the pathogen after 24 h (bacteria) and 48 h (fungi) incubation [20, 21].

The MIC values of the synthesized compounds were determined using dilution techniques, where two (2 ml) millilitres of sterile Mueller Hinton Broth (MHB) for bacterial and potato dextrose broth (PDB) for fungal was added to each test tube followed by dilution of 1 ml from the synthetic sample and was inoculated with the test microorganism and one tube was set up as control with 2 ml of medium and 1 ml of 0.5 Mc Far land standard solution where all the inoculums and all tested tubes were incubated at 37 °C for 24 h (bacterial) and 30 °C (fungal) for 72 h. The test tubes were then checked after the incubation period for growth, where the presence of turbidity indicates the growth, while those resembling to control indicate no growth, while the lowest concentration of the agents that inhibited the visible growth of the tested microbes was recorded as MIC [17].

Result

Characterization of (E)-1-(4-nitrophenyl)-2-(3,4,5-trimethoxybenzylidene) hydrazine for HS6

Dark brown coloured, solid powder product with a percentage yield of 30%. m.p. 161 °C.

The FTIR spectrum of compound **HS6** shows characteristic stretching absorption bands at 3276 cm^{-1}, 1591 cm^{-1}, 1293 cm^{-1}, and 1133 cm^{-1} that indicate the presence of secondary imine group (N–H), azomethine (C = N), N–C, and C–O–C bonds, respectively.

The ^{1}H-NMR spectrum of HS6 exhibited signals at ($CDCl_3$): (δ, ppm) 3.89 (s, 3H, HC-4"), 3.94 (s, 6H, HC-3"/5"), 6.92 (s, 2H, ArHC-2/6), 7.12 (d, 2H, ArHC-2'/6', J = 8 Hz), 7.72 (s, 1H, HC-1"), 8.05 (s, 1H, NH) and 8.19 (d, 2H, ArHC-3'/5', J = 8 Hz).

***The ^{13}C NMR spectrum of HS6, showed signals for sixteen carbon at ($CDCl_3$)*:** (δ, ppm) 55.22 (C-3"/C-5"), 59.82 (C-4"), 102.83 (C-2/C-6), 110.69 (C-2'/C-6'), 125.20 (C-3'/C-5'), 128.60 (C-1), 140.06 (C-4'), 140.12 (C-4), 142.04 (C-1"), 146.56 (C-1') and 152.60 (C-3/C-5).

Characterization of (E)-7-chloro-4-(2-(1-(4-fluorophenyl) ethylidene) hydrazinyl) quinolone HS7

Light golden coloured, solid powder product with percentage yield 38% and M.P. 240.5 °C.

The FTIR spectrum of compound HS7 showed characteristic stretching absorption bands at 3168 cm^{-1}, 1606 cm^{-1}, 1438 cm^{-1}, and 620 cm^{-1} that indicated the presence of secondary imine group (N–H), azomethine (C = N), N–C, and F bonds, respectively.

***The ^{1}H-NMR spectrum of HS7 exhibited signals at (DMSO-d6)*:** (δ, ppm) 2.62 (s, 3H, HC-2"), 7.32 (t, 2H, ArHC-2/6, J = 9 Hz), 7.51 (d, 1H, ArHC-3', 6 Hz), 7.82 (d, 1H, ArHC-6', J = 9 Hz), 8.04 (t, 2H, ArHC-3/5, J = 9 Hz), 8.13 (s, 1H, ArHC-8'), 8.63 (d, 1H, ArHC-6', J = 9 Hz), 8.87 (d, 1H, ArHC-2', J = 9 Hz) and 8.91 (s, 1H, NH).

***The ^{13}C NMR spectrum of HS7, showed signals for eighteen carbon at ($CDCl_3$)*:** (δ, ppm) 16.03 (C-2"), 101.39 (C-3'), 114.88 (C-4"), 116.19 (C-3/C-5), 119.54 (C-6'), 127.31 (C-5'), 129.67 (C-2/C-6), 134.13 (C-1), 138.59 (C-7'), 139.59 (C-8'), 158.52 (C-4'), 161.93 (C-2'), 165.34 (C-4) and 167.08 (C-1").

Synthesis and characterization of (E)-7-chloro-4-(2-(2-(trifluoromethyl) benzylidene) hydrazinyl) quinoline (HS8)

Creamy powder coloured product with percentage yield 57% and m.p. 240.5 °C.

The FTIR spectrum of compound HS8 showed absorption bands at 3339 cm^{-1}, 1613 cm^{-1}, 1587 cm^{-1}, 1312 cm^{-1}, and 620 cm^{-1} that indicated the presence of secondary imine group (N–H), aromatic C = C, azomethine (C = N), N–C, and F bonds, respectively.

***The ^{1}H-NMR Spectrum of HS8 exhibited signals at (DMSO-d6)*:** (δ, ppm) 7.61 (t, 1H, ArHC-3', J-6 Hz), 7.72 (d, 1H, ArHC-4, J = 6 Hz), 7.81 (d, 1H, ArHC-6', J = 6 Hz), 7.87–7.83 (t, 2H, ArHC-3, 5, J = 6, 6 Hz), 7.95 (s, 1H, NH), 8.15 (d, 1H, ArHC-8', J = 3 Hz), 8.39 (d, 1H, ArHC-6, J = 6 Hz), 8.72 (d, 1H, ArHC-5', J = 6 Hz), 8.82 (d, 1H, ArHC-2', J = 6 Hz) and 9.16 (s, 1H).

Carbon nuclear magnetic resonance spectral (*^{13}C-NMR-DMSO-d6)* of compound (HS8) shows the following signal azomethine signals at δ (148.33 ppm) confirming (C = N) while the signal at δ (152.17 ppm) assigned to carbon to nitrogen atoms double (N = C) and the signal at δ (151.73 ppm) referencing for (-N–C) in pyridine ring, respectively, where signal at δ 134.17 ppm due to carbon atom attached to chlorine at position seven of quinoline ring (7-Cl–C-R).

Synthesis and characterization of 1-(3-(4-fluorophenyl)-5-(4-hydroxy-3-methoxyphenyl)-4,5-dihydro-1H-pyrazol-1-yl) ethanone (HS9)

Sandy brown powder coloured product with a percentage yield 10% and a melting point of 173 °C.

The FTIR spectrum of compound HS9 showed absorption bands at 3231 cm^{-1}, 1632 cm^{-1}, 1602 cm^{-1}, 1420 cm^{-1}, and 1218 cm^{-1} that indicated the presence of hydroxyl (OH), amide group (C=O), azomethine (C=N), methoxy group C–O–C, and N–C bonds, respectively.

The ^{1}H-NMR spectrum of HS9 exhibited signals at ($CDCl_3$): (δ, ppm) 2.39 (s, 3H, HC-2^0), 3.13/3.69 (dd, 2H, HC-4a/4b, J=4, 8 Hz), 3.89 (d, 3H, HC-3^0), 5.49 (dd, 1H, HC-3), 6.73–6.67 (tt, 2H, ArHC-2', 3', J=8.16, 1.96 Hz), 6.82 (t, 1H, ArHC-6'), 7.09 (m, 2H, ArHC-3"/5", J=4.8 Hz), 7.24 (s, 1H, OH) and 7.71 (m, 2H, ArHC-2"/6", J=4.8 Hz).

The ^{13}C NMR Spectrum of HS9, showed signals for eighteen carbon at ($CDCl_3$): (δ, ppm) 21.99 (C-2^0), 42.47 (C-4), 55.92 (C-3^0), 59.91 (C-3), 108.63 (C-6'), 114.80 (C-3'), 115.94 (C-3"/C-5"), 118.10 (C-2'), 128.57 (C-2"/C-6"), 133.86 (C-1'), 145.16 (C-4'), 146.63 (C-5'), 152.94 (C-5), 162.73 (C-4") and 168.93 (C-1^0).

Synthesis and characterization 1-(5-(4-hydroxy-3-methoxy phenyl)-3-(4-(methylamino) phenyl)-4,5-dihydro-1H-pyrazol-1-yl) ethanone (HS10)

Light brown powder coloured product with percentage yield 62% and M.P. 226 °C.

The FTIR spectrum of compound HS10 showed absorption bands at 3082 cm^{-1}, 1625 cm^{-1}, 1595 cm^{-1}, 1476 cm^{-1}, and 1252 cm^{-1} that indicated the presence of hydroxy (OH), amide group (C=O), azomethene (C=N), methoxy group C–O–C, and N–C bonds, respectively.

The ^{1}H-NMR Spectrum of HS10 exhibited signals at (CD_3COCD_3): (δ, ppm) 2.41 (s, 3H, HC-4^0), 3.11–3.68 (dd, 2H, C-4a, J=4, 16 Hz), 3.83 (s, 3H, HC-2^0), 3.85 (s, 3H, HC-6^0), 4.53 (s, 1H, NH), 5.5 (t, 1H, HC-3), 6.69 (d, 1H, ArHC-6', J=8 Hz), 6.75 (s, 1H, ArHC-2'), 6.90 (d,1H, ArHC-3"/5", J=8 Hz), 7.0 (d, 1H, ArHC-5' J=8 Hz), 7.25 (s, 1H, OH) and 7.80 (d, 2H, ArHC-2"/6", J=8 Hz).

The ^{13}C NMR spectrum of HS10 showed signals for nineteen carbon at (CD_3COCD_3): (δ, ppm) 20.95 (C-4^0), 41.49 (C-2^0), 54.39 (C-4), 54.94 (C-6^0), 58.67 (C-3), 107.65 (C-2'), 113.21 (C-3"/C-5"), 113.76 (C-5^0), 123.01 (C-6'), 126.02 (C-1"), 127.18 (C-2"/C-6"), 133.00 (C-1'), 144.08 (C-4'), 145.63 (C-3'), 152.93 (C-5), 160.34 (C-4") and 167.84 (C-3^0).

Molecular docking screening

The docking studies were performed to evaluate the binding potential of five synthesized compounds against two target enzymes: bacterial dihydrofolate reductase (DHFR-7REB) and fungal squalene epoxidase (SQLE-6C6P). Ciprofloxacin and terbinafine were used as reference drugs for the bacterial and fungal targets, respectively. The aim was to predict how effectively each ligand fits into the active binding site of the target proteins while docking simulations revealed the strength and nature of the protein–ligand interactions, with binding affinity scores expressed in kcal/mol [23].

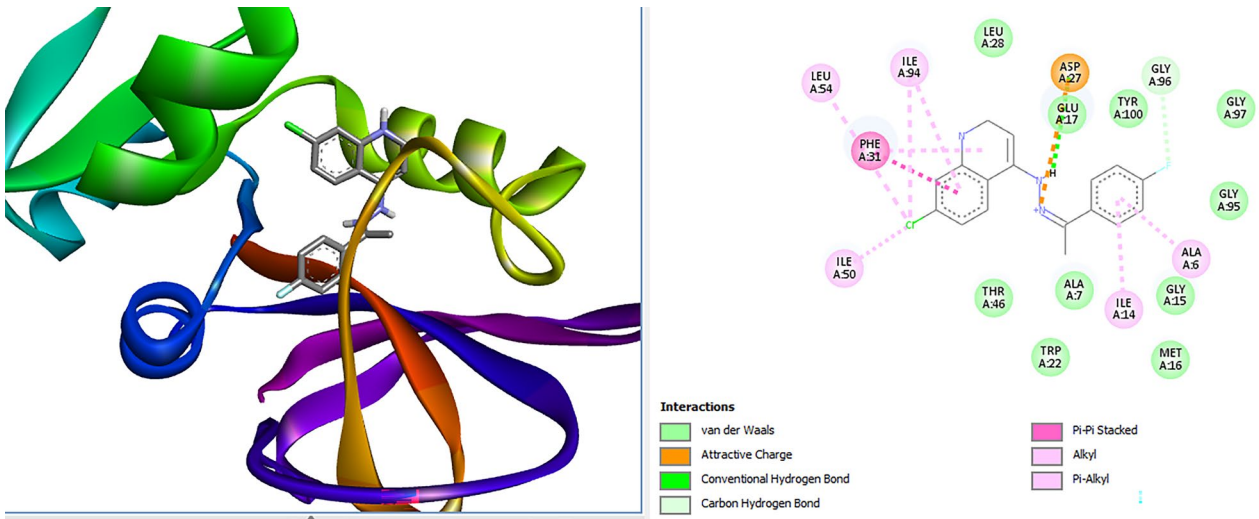

Fig. 1 3D and 2D conformations of HS7 at the active site of the receptor (ID: 7REB)

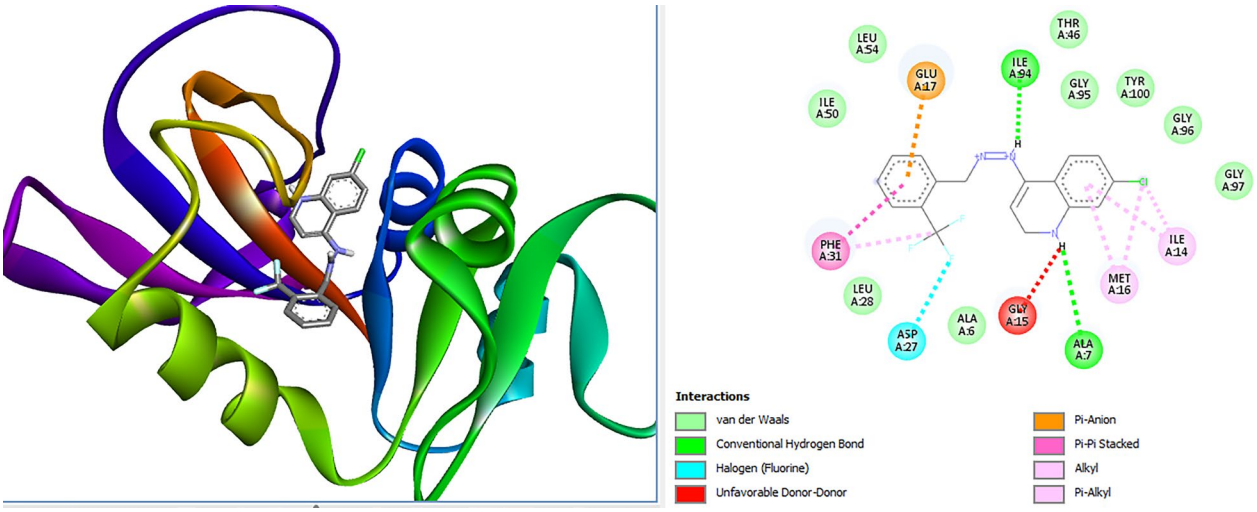

Fig. 2 3D and 2D conformations of HS8 at the active site of the receptor (ID: 7REB)

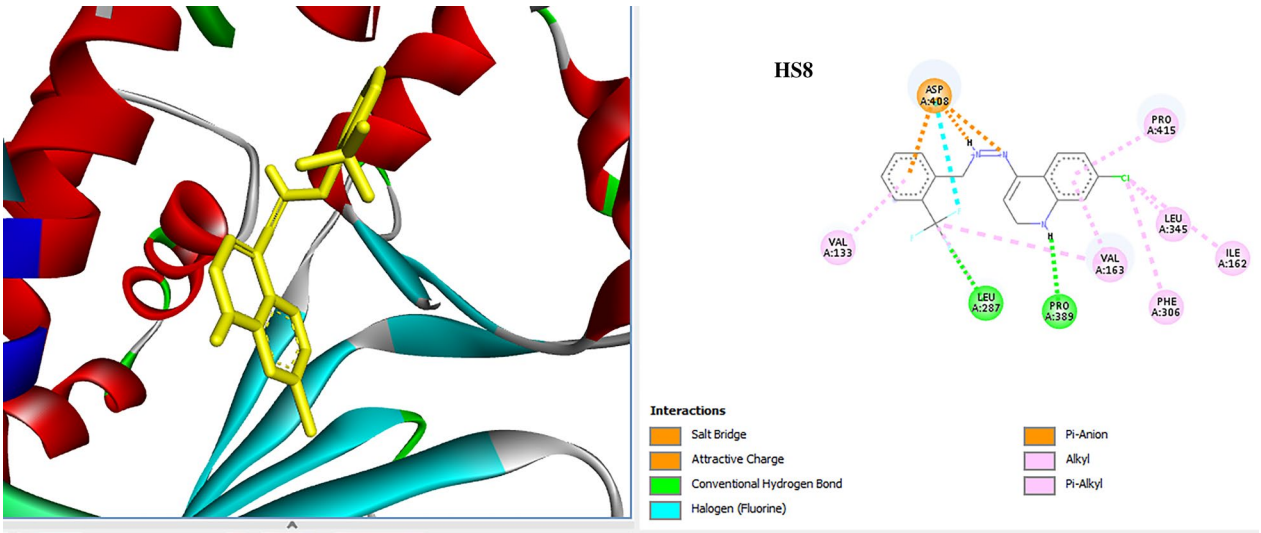

Fig. 3 3D and 2D conformations of compounds HS8 at the active site of the receptor (PDB: 6C6P)

Analysis of binding poses and interactions of the test compounds

Analysis of the highest binding poses and interactions of the selected synthesized compounds of the phenylhydrazone and pyrazoline derivatives was carried out across the two enzymes, as shown in their 3D and 2D relative conformation (Figs. 1, 2, 3, 4, 5).

Discussion

NMR spectra analysis for compound (HS6–HS10)

The ^{1}H-NMR spectra analysis for (HS6) showed seven different proton peaks were observed, and the present of singlet signal (ppm) at δ 6.85 confirmed the formation azomethine (H-C=N). Meanwhile, the ^{13}C-NMR spectra showed the total number of 16 carbon atoms, and the spectrum was confirmed, due to the carbon signals of azomethine carbon (C=N) at 142.04 shown in Table 2.

The ^{1}H-NMR spectral analysis of (HS7) showed eight different proton signals, and the singlet signal at δ (ppm) 2.56 (s) indicated the presence of proton signal of methyl-azomethine (Me-C=N), and the ^{13}C NMR spectral showed the characteristics of carbon signals of an azomethine carbon (C=N) appeared at 167.08 (C-1) as shown in Table 3.

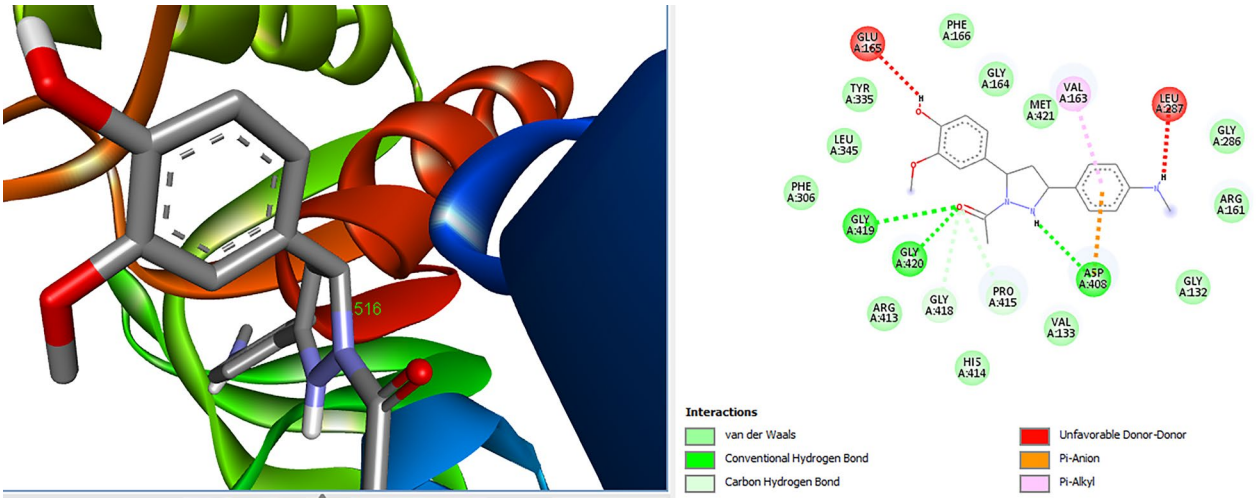

Fig. 4 3D and 2D conformations of compound HS10 at the active site of the receptor (PDB: 6C6P)

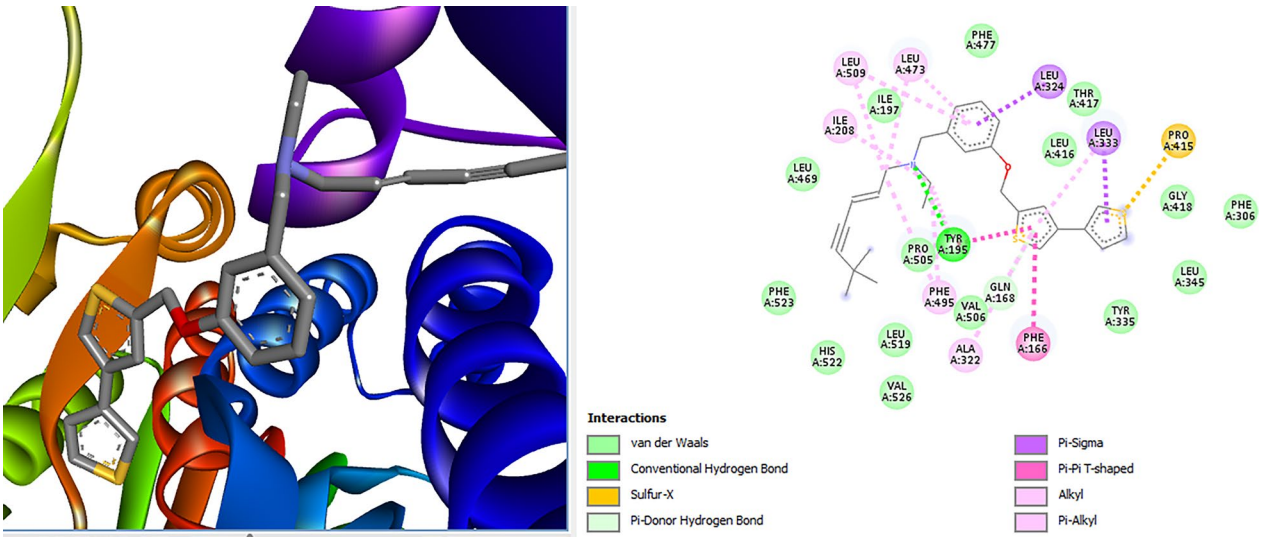

Fig. 5 3D / 2D view of the binding pose of the Co-crystal ligand (EMV) at active site of the SQLE

The ^{1}H-NMR spectral analysis of (HS8) showed ten different proton signals, and the singlet signal at δ (ppm) 3.41 (s) indicated the presence of proton signal of azomethine (H-C=N), while the ^{13}C-NMR spectral showed 16 carbon atoms with the characteristics of carbon signals of an azomethine carbon (C=N) appeared at 153.16 (C-1), shown in Table 4.

The ^{1}H-NMR spectral analysis of (HS9) showed ten different proton signals; meanwhile, the carbonyl methyl appeared as singlet at δ 2.39 ppm and the disappearance of the α,β-unsaturated ketone linker protons signal of chalcone, and appearance of double of doublets at around δ 3.12, 3.68, and 5.5 ppm, for 4-Ha, 4-Hb, and 3-H, respectively; this revealed the confirmation of pyrazoline ring. The presence of aromatic methoxy protons (Ar–OCH_3), methyl protons of the acetyl group, and other proton confirmed the product due to consistent with the values for the substituent attached to aryl rings reported by Ragab work, and the disappearance of α,β-unsaturated protons (from chalcone) and the emergence of new signals confirm cyclization to pyrazoline, consistent with pyrazoline synthesis mechanisms reported by Ragab e*t al.* [25]. The ^{13}C-NMR spectral showed the characteristics of carbon signals; the presence of chemical shift values at 168.93 ppm and 21.98 ppm (C=O and CH_3) confirmed the presence of carbonyl moiety in the acetyl fragment attached to the pyrazoline ring shown in Table 5. The spectrum of HS9, the peaks observed strongly confirmed

Table 2 Zone of inhibition (mm) of the target compounds HS6–HS10

	Conc	Gram-positive bacteria			Gram-negative bacteria			Fungi
Entry	(mg/ml)	*S. aureus*	*B. subtilis*	*S.pneumonia*	*E. coli*	*S. Typhi*	*Ps. aeruginosa*	*A. niger*
HS6	50	17	17	18	20	20	19	15
	25	14	14	15	17	17	16	0
	12.5	12	12	12	14	13	13	0
HS7	50	14	15	14	13	14	13	12
	25	0	12	0	0	0	0	0
	12.5	0	0	0	0	0	0	0
HS8	50	14	16	17	17	17	14	12
	25	0	12	13	13	14	0	0
	12.5	0	0	0	0	0	0	0
HS9	50	14	18	14	13	18	14	13
	25	0	16	0	0	15	0	0
	12.5	0	0	0	0	0	0	0
HS10	50	16	16	14	14	17	15	12
	25	13	13	0	0	14	12	0
	12.5	0	0	0	0	0	0	0
CF/TN	10/30	30	36	35	22	35	37	30

CF ciprofloxacin, *TN* terbinafine as reference drugs

Table 3 Minimal inhibitory concentrations (MICs mg/mL) of the target compounds HS6–HS10

Test organism	Gram-positive bacteria			Gram-negative bacteria			Fungi
	S.aureus	*B.subtilis*	*S. pneum*	*E. coli*	*S. typhi*	*Ps. aeruginosa*	*A. niger*
HS6	25	25	12.5	12.5	12.5	12.5	50
HS7	50	50	50	NI	50	NI	NI
HS8	50	25	25	25	25	50	NI
HS9	50	25	50	NI	25	50	NI
HS10	25	25	50	50	25	50	NI

NI mean no inhibition

Table 4 Minimal bactericidal concentrations (MBCs mg/mL) of the target compounds HS6–HS10

Test organism	Gram-positive bacteria			Gram- negative bacteria		
	S. aureus	*B. subtilis*	*S.pneumonia*	*E. coli*	*S. typhi*	*Ps. Aeruginosa*
HS6	50	50	50	25	25	25
HS7	NI	NI	NI	NI	NI	NI
HS8	NI	50	50	50	50	NI
HS9	NI	50	NI	NI	50	NI
HS10	50	50	NI	NI	50	NI

NI mean no inhibition

the product based on previous reported data on structurally analogous pyrazoline systems.

The ^{1}H-NMR spectra analysis of (HS10) showed ten different characteristic of proton signals, proton signal methyl attached to amine group which was observed around ppm 2.83 while carbonyl methyl appeared as singlet at δ 2.41 ppm and the disappearance of the α,β-unsaturated ketone linker protons signal of chalcone and appearance of double of doublets at around δ 3.16, 3.84, and 5.52 ppm, for 4-Ha, 4-Hb, and 3-H, respectively;

Table 5 Physicochemical parameters of the synthesized compounds HS6–HS10

Entry	MW[a]	LogP[b]	HBA[c]	HBD[d]	RB[e]	L.Violation	TPSA (Ă)[f]	[g]BA Score
HS6	331.32	1.24	6	1	7	0	97.90	0.55
HS7	313.76	3.86	3	1	3	0	32.28	0.55
HS8	349.74	4.09	3	1	4	0	37.28	0.55
HS9	328.34	2.43	5	1	4	0	62.13	0.55
HS10	339.39	2.43	6	2	5	0	74.16	0.55
Lip	≤ 500	≤ 5	≤ 10	≤ 5	≤ 10	≤ 1	≤ 140	> 0.1

a Molecular weight (MW)

b Logarithm of partition coefficient between n-octanol and water (LogP)

c Number of Hydrogen bond acceptors (HBA)

d Number of hydrogen bond donors (HBD)

e Number of rotatable bonds (RB)

f Topological polar surface area (TPSA)

g Bioavailability (BA), L. Lipinski's rules of 5

this revealed the confirmation of pyrazoline ring. Importantly, the disappearance of the α,β-unsaturated proton signals typical of chalcone and appearance of new aliphatic signals between δ 3.1 and 5.5 ppm confirmed the successful cyclization of the chalcone to pyrazoline, in agreement with the literature reported by [26, 27]. ^{13}C-NMR spectral showed 19 carbon atoms from different rings A, B, and C, and the structure of pyrazoline showed the chemical shift values at 167.84 ppm indicate the presence of (C = O) the carbonyl moiety in the acetyl fragment attached to the pyrazoline ring. All the data provided above correspond well with previously reported pyrazoline derivatives bearing methoxy and hydroxyl substitutions [28, 29]. The combination of FTIR, ^{1}H-NMR, and ^{13}C-NMR spectroscopic data provided strong evidence for the successful formation of the scaffold (HS9 and HS10) which revealed the absence of chalcone-linked unsaturation and the appearance of characteristic pyrazoline resonances clearly demonstrate cyclization confirming the ring closure into a pyrazoline scaffold [27].

Antimicrobial evaluation

The synthesized compounds HS6–HS10 exhibited low to moderate antibacterial inhibition zone with values range (12–20 mm) and antifungal (12–15 mm) activities against selected Gram-positive (S. *aureus*, *B. subtilis*, *S. pneumoniae*), Gram-negative (E. *coli*, *S. Typhi*, *P. aeruginosa*), and fungal (*A. niger*) strains. Compared to the standard drugs ciprofloxacin and terbinafine (22–37 mm), the test compounds were generally less potent at equivalent concentrations. Among the synthesized compound, **HS6**, having a biaryl hydrazone bearing electron-donating methoxy groups and a strong electron-withdrawing nitro group, demonstrated the highest antimicrobial activity, especially at the lowest tested concentration (12.5 μg/mL), suggesting favourable electronic synergy enhancing its bioactivity, but still compound HS6 also showed the best antifungal activity at 50 μg/mL, while the remaining compounds were found inactive at lower antifungal concentrations. However, for the quinoline-based series, **HS8** outperformed **HS7**, likely due to the presence of a trifluoromethyl group (CF_3) at the ortho-position, which may enhance metabolic stability and membrane permeability. The literature supports the role of ortho-fluorination in improving antibacterial activity through electronic and steric effects. Meanwhile, the pyrazoline derivatives, particularly for compound **HS9** and **HS10**, displayed moderate antibacterial activity with inhibition zone value range (13–17 mm) revealing weak effects against certain strains (*S. aureus*, *B. subtilis*, *S. Typhi*), with limited antifungal efficacy. The structure–activity relationship suggests that the nature and position of substituents on the aromatic rings significantly influence antimicrobial potency, with electron-donating/withdrawing combinations and fluorine substitutions playing key roles.

Comparison of MIC and MBC values of synthesized agents (HS6–HS10) to the reference Standard of ciprofloxacin

In the present study, ciprofloxacin was used as the standard reference drugs due to its established broad-spectrum bactericidal activity and the reference drugs ciprofloxacin exhibited an MIC of 0.125 mg/mL and an MBC of 0.5 mg/mL against the tested bacterial strains, corresponding to an MBC/MIC ratio of 4, indicating the bactericidal effect.

Effect of the synthesized compound when compared to reference standard:

- The HS6 showed the broadest antibacterial spectrum among the synthesized agents, with MIC val-

ues ranging from 12.5 to 25 mg/mL and MBC values from 25 to 50 mg/mL against both Gram-positive and Gram-negative bacteria. Although these values are significantly higher (≈100–200-fold) than ciprofloxacin, HS6 maintained an MBC/MIC ratio ≤ 4 for all susceptible strains, indicating bactericidal activity.

- HS7 was largely inactive, with MICs of 50 mg/mL against only a few strains (*S. aureus*, *B. subtilis*, *S. pneumoniae*, *S. typhi*) and no detectable MBC within the tested range, in contrast with the potent activity of ciprofloxacin.
- HS8 displayed moderate activity, with MICs of 25–50 mg/mL and MBC values of 50 mg/mL for most susceptible strains (*B. subtilis*, *S. pneumoniae*, *E. coli*, *S. typhi*), yielding MBC/MIC ratios of 2 (bactericidal). However, activity was absent against *S. aureus* and *P. aeruginosa*.
- HS9 exhibited selective bactericidal activity against *B. subtilis* and *S. typhi* (MIC = 25 mg/mL, MBC/MIC = 2) but was inactive against several strains including *S. aureus*, *S. pneumoniae*, and *P. aeruginosa*.
- HS10 showed similar activity to HS6 against Gram-positive bacteria (MIC = 25 mg/mL, MBC/MIC = 2) but limited action against Gram-negative species, with inactivity against *P. aeruginosa* and *S. pneumoniae*.

Generally, all the synthesized agents were considerably less potent than ciprofloxacin in terms of MIC and MBC values, but HS6 demonstrated the widest spectrum of bactericidal activity, followed by HS8 and HS10. HS7 and HS9 showed narrow-spectrum activity. However, these findings suggest that the synthesized agents possess antibacterial potential, with substantial structural optimization needed to improve potency to clinically relevant steps.

In silico physicochemical parameter evaluation

The physicochemical properties of the synthesized phenylhydrazone and pyrazoline derivatives were assessed using the SwissADME web-based tool. Key descriptors evaluated included molecular weight, number of hydrogen bond donors (HBD), number of hydrogen bond acceptors (HBA), number of rotatable bonds, and lipophilicity, represented as MLogP. These parameters were analysed in accordance with **Lipinski's rule of five**, a well-established guideline used to predict oral bioavailability and assess drug-likeness. All five synthesized compounds complied with the Lipinski criteria, with each parameter falling within the acceptable range. This compliance indicates that the compounds exhibit favourable physicochemical profiles, supporting their potential as viable candidates for further development as orally active antimicrobial agents shown in Table 3 [5].

Virtual toxicity assessment

Virtual toxicity prediction provides a valuable approach for assessing the potential adverse effects of chemical compounds on human health by simulating drug–target interactions at the molecular level. This method offers significant advantages over traditional *in-vivo* toxicity testing, including reduced costs, shorter evaluation times, and the elimination of ethical concerns related to animal use and also serves as a complementary tool to conventional toxicity studies which supports early-stage decision-making in drug development [22]. In the present study, a virtual toxicity assessment was performed on the five synthesized phenylhydrazone and pyrazoline derivatives to evaluate their potential for hepatotoxicity, mutagenicity, carcinogenicity, cytotoxicity, and immunotoxicity (Table 4). These endpoints were selected based on their relevance to common drug safety concerns in clinical applications. The predicted results indicated that all five compounds exhibited favourable toxicity profiles, with no significant alerts for major toxicological endpoints. Notably, compounds HS7 and HS10 demonstrated low toxicity risks across all evaluated parameters, suggesting their potential as safe candidates for further preclinical development.

This in silico approach also allows for both qualitative (binary active/inactive classification) and quantitative (e.g. LD_{50} values) prediction of toxicity outcomes, making it a robust tool in early toxicity screening. However, this finding supports the utility of computational methods as effective predictive models in the assessment of chemical safety during the early phases of drug discover [4].

Validation of docking procedure

The molecular docking protocols employed for both target enzymes were rigorously validated to ensure their reliability and predictive accuracy. As presented in Table 6, the co-crystallized ligands were re-docked into the active sites of their respective protein structures. The re-docked conformations, shown in cyan, exhibited a high degree of superimposition with their original poses as retrieved from the Protein Data Bank (PDB). This strong alignment indicates that the docking methodology is capable of accurately reproducing experimentally observed binding modes. Consequently, this validation supports the suitability of the docking procedure for evaluating the binding interactions of the synthesized compounds with the enzyme active sites, thereby enhancing the credibility of subsequent in silico predictions [22]

Table 6 In silico toxicity prediction of synthesized phenylhydrazone and pyrazoline derivatives on selected human toxicological endpoints

Code	LD50 mg/kg	Toxicity class	Cytoxicity	Carcinotoxicity	Hepatoxicity	Immunotoxicity
HS6	800	4	Inactive (0.58)	Active (0.58)	Active (0.59)	Active (0.96)
HS7	1000	4	Inactive (0.83)	Inactive (0.55)	Active (0.61)	Active (0.98)
HS8	1250	4	Inactive (0.79)	Inactive (0.54)	Active (0.62)	Active (0.99)
HS9	1880	4	Inactive (0.74)	Inactive (0.51)	Active (0.58)	Active (0.71)
HS10	1000	4	Inactive (0.76)	Active (0.62)	Active (0.55)	Inactive (0.75)

Active / inactive predicted the probability range, indicating harmful or safe within the acceptable value range

Drug Intermolecular interaction and binding affinity

The molecular docking studies were conducted using Discovery Studio Visualizer against two key microbial targets (enzymes): dihydrofolate reductase with PDB ID (7REB) and human squalene epoxidase with PDB ID (6C6P). Among the tested ligands, both HS7 and HS8 showed the strongest binding affinities against target enzymes 7REB with docking scores of -9.6 and -9.4 kcal/mol, respectively, outperforming the reference drug ciprofloxacin (-7.4 kcal/mol), while for the 6C6P target enzymes, the ligands HS8 (-10.2 kcal/mol) and HS10 (-9.8 kcal/mol) demonstrated the highest affinities, comparable to reference drug terbinafine (-9.8 kcal/mol). However, compound HS8 exhibited the strongest binding for both targets enzymes. Meanwhile, the ligand

Table 7 Docking validation for the crystal structure of enzyme complexes (left view) and re-docked ligand superimposed (right view)

Enzyme	Crystal structure complex (enzyme and ligand)	Crystal structure complex with re-docked ligand (validation)
7REB	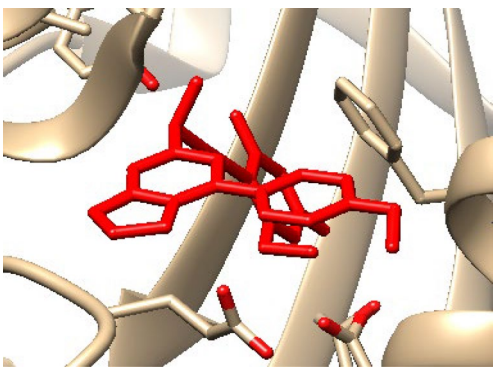	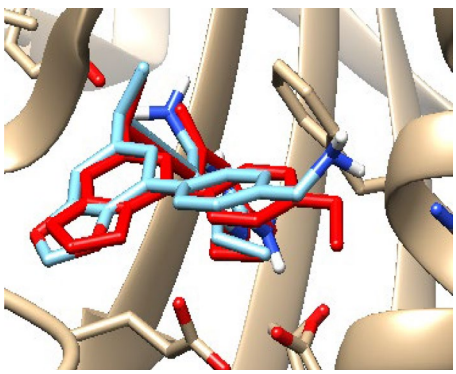
6C6P	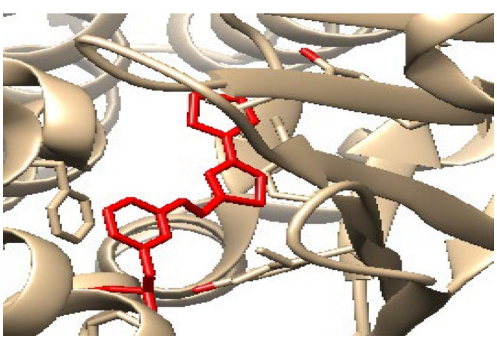	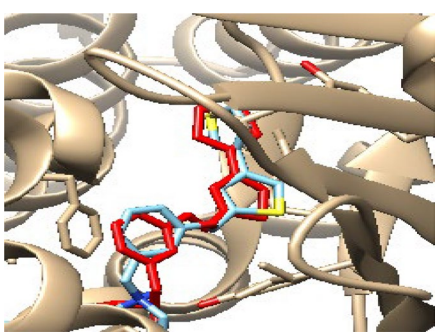

Re-docked validation of the co-crystallized ligand in red colour highlighted molecule

HS7 formed key interactions with 7REB, including a conventional hydrogen bond with ASP27 (2.93 Å), a carbon–hydrogen bond with GLY96 (2.83 Å), and multiple hydrophobic contacts with ILE50, LEU50, ALA6, and PHE31. Additionally, an ionic interaction with ASP27 (4.70 Å) was observed, and compound HS8 displayed two conventional hydrogen bonds (ILE94 and ALA7), a halogen bond with ASP27 (3.18 Å), and π–π stacking with PHE31. In conclusion, the interactions suggest that the HS7 and HS8 are strong candidates for inhibiting DHFR, while HS8 and HS10 show promising antifungal potential via SQLE inhibition (Table 7).

Biochemical and cellular assays corroborated the docking predictions, demonstrating that ligands HS7–HS8 inhibited bacterial DHFR *in vitro* (IC_{50} in the low-μM range), with CETSA and folate metabolite profiling confirming target engagement and pathway disruption, as further supported by thymidine rescue of antimicrobial activity. Similarly, HS8 and HS10 inhibited squalene epoxidase (IC_{50} comparable to terbinafine), induced the expected sterol profile (squalene accumulation and ergosterol depletion), and exhibited partial ergosterol rescue in fungal growth assays, collectively validating the DHFR inhibition by HS7–HS8 and SQLE inhibition by HS8 and HS10.

Conclusion

In summary, the present study reports the successful synthesis and characterization of a series of novel (E)-substituted N-phenylhydrazone, quinoline-based hydrazones, and pyrazoline derivatives, evaluated for their antimicrobial potential through both in vitro and in silico approaches. Among the five synthesized compounds (HS6–HS10), three of the derivatives (HS6, HS7, and HS8) demonstrated appreciable antimicrobial activity, particularly against a spectrum of Gram-positive and Gram-negative bacteria, as well as fungal strains. Notably, compound HS6 exhibited the most potent inhibitory activity across multiple bacterial strains, including drug-resistant pathogens, and was the only compound that retained activity at the lowest tested concentration (12.5 μg/mL), underscoring its promising therapeutic potential.

The in silico molecular docking studies targeting dihydrofolate reductase (DHFR, PDB ID: 7REB) and squalene epoxidase (SQLE, PDB ID: 6C6P) revealed strong binding affinities for HS7, HS8, and HS10, with HS8 demonstrating dual-targeting capability and superior binding scores relative to standard drugs ciprofloxacin and terbinafine. These interactions were supported by favourable hydrogen bonding, hydrophobic, ionic, and π-stacking interactions within the active sites of the respective receptors.

Furthermore, ADMET profiling via virtual screening confirmed that all compounds comply with Lipinski's rule of five, suggesting good oral bioavailability and drug-likeness with low toxicity risk. The observed structure–activity relationships (SAR) highlighted the influence of electron-donating and electron-withdrawing substituents, particularly the combination of trimethoxy and nitro groups (HS6), and the ortho-trifluoromethyl group (HS8), in enhancing antimicrobial efficacy.

Overall, these findings suggest that the (E)-phenylhydrazone and pyrazoline scaffolds investigated in this work, especially HS6 and HS8, serve as promising leads for further optimization and development of new antimicrobial agents targeting resistant bacterial and fungal pathogens.

Abbreviations

MIC	Minimal inhibitory concentration
ZOI	Zone of inhibition
MBC	Minimum bactericidal concentration
MFC	Minimum fungicidal concentration
FTIR	Fourier transform infrared
NMR	Nuclear magnetic resonance
1D	One-dimensional
2D	Two-dimensional
HS6–HS10	Synthetic hydrazone and pyrazoline derivatives (symbolic code number)

Acknowledgements

The author extends sincere gratitude to his supervisors for their exceptional mentorship and unwavering support throughout the course of this research. Special thanks also go to the academic and technical staff of the Faculty of Pharmaceutical Sciences, Ahmadu Bello University, Zaria, for their valuable assistance, encouragement, and provision of laboratory facilities, which significantly contributed to the success of this work and department of Chemistry, University of Pretoria, Republic of South Africa, for using their support in conducting NMR spectral analysis.

Author Contributions

I, Dr. Rabiu Bako designed and conducted the synthesis of phenylhydrazone and pyrazoline derivatives, performed the antimicrobial assays, analyzed the data, and drafted the manuscript under the supervision of Dr. Natasha, October, Prof. Abdullahi, Yunusa, Idris, Dr. Asma'u, Nasir, Hamza3, Prof. Gbonjubola, Olusesi, Adeshina, contributed to study design, guided data interpretation, and critically revised the manuscript for important intellectual content. The Dr. Ahmed, Rufa'i, Pharm. Isah, Jamiu, Muhammad and Dr.Yahaya, Yakubu are collaborator's assisted in spectral characterization and contributed to manuscript editing. All authors read and approved the final manuscript.

Funding

This research was supported by the Tertiary Education Trust Fund (TETFund), Nigeria, through Kaduna State University.

Data Availability Statement

The datasets generated and analyzed during the current study are included in this published article and its supplementary materials. Additional data are available from the corresponding author upon reasonable request.

Declarations

Competing interests

The authors declare that they have no competing interests.

Author details
[1]Department of Pharmaceutical and Medicinal Chemistry, Faculty of Pharmaceutical Sciences, Kaduna State University, Tafawa Balewa Way, PMB 2339, Kaduna, Kaduna State, Nigeria. [2]Department of Chemistry, University of Pretoria, Pretoria, Republic of South Africa. [3]Department of Pharmaceutical and Medicinal Chemistry, Ahmadu Bello University Zaria, Zaria, Kaduna State, Nigeria. [4]Department of Pharmaceutical Microbiology, Ahmadu Bello University Zaria, Zaria, Kaduna State, Nigeria. [5]Department of Pharmaceutical and Medicinal Chemistry, Gombe State University, Gombe, Gombe State, Nigeria. [6]Department of Pharmaceutical and Medicinal Chemistry, Ibrahim Badamasi Babangida State University Lapai, Lapai, Niger State, Nigeria. [7]Department of Pure and Applied Chemistry, Kaduna State University, Kaduna, Kaduna State, Nigeria. [8]Kaduna State University, KASU, Kaduna, Nigeria.

Received: 18 June 2025 Accepted: 12 September 2025
Published online: 25 September 2025

References

1. Mandal SP, Kundu M (2021) An overview on impact of electromagnetic radiations on environment and human health. Res Rev Int J Multidiscip 6(6):3079–3083. https://doi.org/10.31305/rrijm.2019.v04.i03.695
2. Breijyeh Z, Karaman R (2023) Design and synthesis of novel antimicrobial agents. Antibiotics. https://doi.org/10.3390/antibiotics12030628
3. Salem MA, Ragab A, El-Khalafawy A, Makhlouf AH, Askar AA, Ammar YA (2020) Design, synthesis, in vitro antimicrobial evaluation and molecular docking studies of indol-2-one tagged with morpholinosulfonyl moiety as DNA gyrase inhibitors. Bioorg Chem 96:103619. https://doi.org/10.1016/J.BIOORG.2020.103619
4. Liu XJ et al (2023) Recent development of multi-target VEGFR-2 inhibitors for the cancer therapy. Bioorg Chem. https://doi.org/10.1016/j.bioorg.2023.106425
5. Sadeghian S, Zare F, Goshtasbi G, Fassihi A, Saghaie L, Zare P, Sabet R (2023) Synthesis, antimicrobial evaluation, molecular docking, and adme studies of some novel 3-hydroxypyridine-4-one derivatives. Chem Sel 8(44):e202302408
6. Nesterkina M, Barbalat D, Kravchenko I (2020) Design, synthesis and pharmacological pro fi le of (−) - verbenone hydrazones. Open Chem. https://doi.org/10.1515/chem-2020-0103
7. O. T. Synthesis, "Egyptian Journal of Chemistry," vol. 65, no. 10, pp. 239–248, 2022, https://doi.org/10.21608/EJCHEM.2022.129819.5727.
8. Tok F, Doğan MO, Gürbüz B, Kaymakçıoğlu B (2022) Synthesis of novel pyrazoline derivatives and evaluation of their antimicrobial activity. J Res Pharm 26(5):1453–1460
9. Al-Otibi F, Alkhudhair SK, Alharbi RI, Al-Askar AA, Aljowaie RM, Al-Shehri S (2021) The antimicrobial activities of silver nanoparticles from aqueous extract of grape seeds against pathogenic bacteria and fungi. Molecules 26(19):6081
10. Arshad M, Shoeb M, Shahab K, Asghar A, Dabeer N (2019) benzeneamine: synthesis, characterization, antibacterial, and MTT assessment. SN Appl Sci 1(6):1–8. https://doi.org/10.1007/s42452-019-0571-8
11. Moussa Z, Al-Mamary M, Al-Juhani S, Ahmed SA (2020) Preparation and biological assessment of some aromatic hydrazones derived from hydrazides of phenolic acids and aromatic aldehydes. Heliyon 6(9):e05019
12. Fen K, Dergisi B, Derivatives H 2023 Karadeniz Fen Bilimleri Dergisi. vol 13, no 1, pp 135–152. https://doi.org/10.31466/kfbd.1184337.
13. Candéa ALP et al (2009) Bioorganic & medicinal chemistry letters synthesis and antitubercular activity of 7-chloro-4-quinolinylhydrazones derivatives. Bioorg Med Chem Lett 19(22):6272–6274. https://doi.org/10.1016/j.bmcl.2009.09.098
14. Pavani TFA, Cirino ME, Teixeira TR, De Moraes J, Rando DGG (2023) Targeting the Schistosoma mansoni nutritional mechanisms to design new antischistosomal compounds. Sci Rep. https://doi.org/10.1038/s41598-023-46959-3
15. El-naggar M, Rashdan HRM, Abdelmonsef AH (2023) Cyclization of chalcone derivatives: design, synthesis, in silico docking study, and biological evaluation of new quinazolin-2, 4- diones incorporating five -, six -, and seven-membered ring moieties as potent antibacterial inhibitors. ACS Omega. https://doi.org/10.1021/acsomega.3c02478
16. Wahyuningsih TD, Suma AAT, Astuti E (2019) Synthesis, anticancer activity, and docking study of N-acetyl pyrazolines from veratraldehyde. J Appl Pharm Sci 9(3):014–020
17. Agrawal P, Jeyabalan G 2017 Indian Journal of Pharmaceutical and Biological Research (IJPBR) Synthesis and antimicrobial activity of some newer semicarbazone analogues. vol 5, no 2, pp 12–17
18. Le Thoa NT, Nam PC, Nhat DM (2015) Antibacterial activities of the extracts of *Mimosa pudica* L. an in-vitro study. Int J Adv Sci Eng Inf Technol 5(5):358–361
19. Elhady HA, Al-Nathali HS, El-Sayed R 2017 ISSN : 2320–5407 Manuscript info abstract introduction : - ISSN : 2320–5407 Results and discussion : -. 5:10 1716–1725 https://doi.org/10.21474/IJAR01/5694.
20. You A, Be MAY, In I 2021 Microwave-assisted synthesis and antioxidant activity of an imine , (E) -1- (3- bromobenzylidene) -2-phenylhydrazine Microwave-Assisted Synthesis and Antioxidant Activity of. vol 040041:2020
21. Ade A, Amengor CDK, Brobbey A, Ayensu I, Harley BK, Boakye YD (2020) Synthesis and antimicrobial resistant modulatory activity of 2, 4-dinitrophenylhydrazone derivatives as agents against some ESKAPE human pathogens. J Chem. https://doi.org/10.1155/2020/2720697
22. Banerjee P, Eckert AO, Schrey AK, Preissner R (2018) ProTox-II: a webserver for the prediction of toxicity of chemicals. Nucleic Acids Res 46:257–263
23. Ugbe FA, Abdulkadir I (2022) Molecular docking screening and pharmacokinetic studies of some Boron-Pleuromutilin analogues against possible targets of *Wolbachia pipientis*. J Mol Docking 2(1):29–43
24. Khan MKA, Akhtar S (2023) Novel drug design and bioinformatics: an introduction. Phys Sci Rev. https://doi.org/10.1515/psr-2018-0158
25. Ragab A, Elsisi DM, Abu OA, Abusaif MS, Askar AA, Farag AA, Ammar YA (2022) Design, synthesis of new novel quinoxalin-2 (1 H) - one derivatives incorporating hydrazone, hydrazine, and pyrazole moieties as antimicrobial potential with in-silico ADME and molecular docking simulation. Arab J Chem 15(1):103497
26. Asad M, Arshad MN, Khan SA, Oves M, Khalid M, Asiri AM, Braga AAC (2019) Cyclization of chalcones into N-propionyl pyrazolines for their single crystal X-ray, computational and antibacterial studies. Journal of Molecular Structure, 127186.
27. Selvam S, Arumugam K, Bharathi B, Manivannan R, Subbaiya R (2021) Design and characterization of novel pyrazoline derivatives: NMR, docking, and biological studies. Eur J Med Chem 215:113280
28. Khan KM et al (2020) Hydrazone scaffolds as emerging class of antibacterial agents: synthesis, SAR, and molecular docking studies. Curr Med Chem 27(20):3219–3245
29. Mamand SO, Abdul D, Hawaiz F (2022) Traditional, one pot three component synthesis and anti-bacterial evaluations of some new pyrazoline derivatives. Egypt J Chem 65(10):239–248

Publisher's Note